ORIGINAL ARTICLE

Regional Cerebral Blood Flow and Metabolic Rate in Persistent Lyme Encephalopathy

Brian A. Fallon, MD; Richard B. Lipkin, BA; Kathy M. Corbera, MD; Shan Yu, PhD; Mitchell S. Nobler, MD; John G. Keilp, PhD; Eva Petkova, PhD; Sarah H. Lisanby, MD; James R. Moeller, PhD; Iordan Slavov, PhD; Ronald Van Heertum, MD; Brett D. Mensh, MD, PhD; Harold A. Sackeim, PhD

Context: There is controversy regarding whether objective neurobiological abnormalities exist after intensive antibiotic treatment for Lyme disease.

Objectives: To determine whether patients with a history of well-characterized Lyme disease and persistent cognitive deficit show abnormalities in global or topographic distributions of regional cerebral blood flow (rCBF) or cerebral metabolic rate (rCMR).

Design: Case-controlled study.

Setting: A university medical center.

Participants: A total of 35 patients and 17 healthy volunteers (controls). Patients had well-documented prior Lyme disease, a currently reactive IgG Western blot, prior treatment with at least 3 weeks of intravenous cephalosporin, and objective memory impairment.

Main Outcome Measures: Patients with persistent Lyme encephalopathy were compared with age-, sex-, and education-matched controls. Fully quantified assessments of rCBF and rCMR for glucose were obtained while subjects were medication-free using positron emission tomography. The CBF was assessed in 2 resting room air conditions (without snorkel and with snorkel) and 1 challenge condition (room air enhanced with carbon dioxide, ie, hypercapnia).

Results: Statistical parametric mapping analyses revealed regional abnormalities in all rCBF and rCMR measurements that were consistent in location across imaging methods and primarily reflected hypoactivity. Deficits were noted in bilateral gray and white matter regions, primarily in the temporal, parietal, and limbic areas. Although diminished global hypercapnic CBF reactivity ($P < .02$) was suggestive of a component of vascular compromise, the close coupling between CBF and CMR suggests that the regional abnormalities are primarily metabolically driven. Patients did not differ from controls on global resting CBF and CMR measurements.

Conclusions: Patients with persistent Lyme encephalopathy have objectively quantifiable topographic abnormalities in functional brain activity. These CBF and CMR reductions were observed in all measurement conditions. Future research should address whether this pattern is also seen in acute neurologic Lyme disease.

Arch Gen Psychiatry. 2009;66(5):554-563

Author Affiliations:
Departments of Psychiatry (Drs Fallon, Corbera, Yu, Keilp, Petkova, Lisanby, Moeller, Slavov, Mensh, and Sackeim), Radiology (Drs Van Heertum and Sackeim), and Biostatistics (Dr Petkova), College of Physicians and Surgeons of Columbia University, New York, New York; the New York State Psychiatric Institute, New York (Drs Fallon, Corbera, Yu, Nobler, Keilp, Petkova, Lisanby, Moeller, Slavov, Mensh, and Sackeim); the Department of Neural and Behavioral Science, State University of New York at Downstate, New York (Mr Lipkin); and the Department of Psychiatry and Behavioral Sciences, New York Medical College, New York (Dr Nobler).

LYME DISEASE, A MULTISYSTEMIC infection caused by the spirochete *Borrelia burgdorferi*, can affect many organs including the central nervous system (CNS). While most patients recover fully when treated with antibiotics soon after infection, patients who are treated months after the initial infection may sustain ongoing problems with fatigue, cognition, and pain despite receipt of a standard course of antibiotics.[1,2] These patients have been described as having chronic Lyme Disease or posttreatment Lyme disease syndrome.[3,4] Continuing symptoms have been attributed to persistent infection,[3] pathogen-induced autoimmunity,[5] or unrelated processes such as depression, somatization, fibromyalgia, or chronic fatigue syndrome.[4] Objective markers of disease are needed.

Structural imaging studies with magnetic resonance imaging (MRI) in acute neurologic Lyme disease have demonstrated white matter hyperintensities on T2-weighted images similar to those seen in demyelinating or inflammatory disorders.[6,7] In patients with later-stage neurologic Lyme disease, initial reports indicated that these hyperintensities persist after treatment, but are less prevalent or severe.[8] However, a recent age- and sex-matched control study revealed that patients with later stage Lyme disease do not have a higher frequency of white matter hyperintensities or basal ganglia lesions.[9]

In functional imaging studies, hypoperfusion has been reported in small case series of patients with chronic Lyme disease using brain single-photon emission computed tomography (SPECT). Characterized by widely distributed multifocal

areas of decreased perfusion in both cortical and subcortical white matter, this pattern is typical of patients with cerebral vasculitis or encephalitis.[10] A case-control study using technetium 99m SPECT compared cognitively impaired patients with Lyme disease with older healthy controls and found multifocal areas of hypoperfusion in the subcortical frontotemporal white matter and basal ganglia as well as in the frontal cortex and cingulate gyrus.[11] Another study compared posttreatment patients with Lyme disease with carefully matched archived controls using the fully quantitative xenon^{133} inhalation technique (external detector system).[12] Significant cerebral blood flow (CBF) reductions were noted in compartment-modeled flows primarily reflecting white matter perfusion, particularly in bilateral posterior temporal and parietal lobes.

In the only prior study of brain metabolism in Lyme disease, 23 patients received positron emission tomography (PET) measurement of regional cerebral metabolic rate (rCMR) for glucose.[13] Qualitative clinical readings revealed hypometabolism in 74% of the patients' temporal lobes, but in a subset of these, the frontal and parietal lobes were also affected. However, criteria for diagnosis of Lyme disease were unclear and this study did not include matched healthy comparison subjects.

This limited literature suggests that while structural abnormalities are not likely to be found in chronic Lyme disease, regional functional abnormalities in rCBF and rCMR may be seen. However, each of these functional studies had design limitations that preclude definitive conclusions. Further, no study has yet assessed both cerebral metabolism and blood flow in the same set of patients.

The purpose of this study was to address the lack of systematic data regarding rCBF and rCMR in patients with persistent Lyme encephalopathy, a type of chronic Lyme disease characterized by cognitive deficits that persist or return after antibiotic treatment. In this study, carefully characterized patients were compared with age-, sex-, and education-matched healthy volunteers (controls) using a series of PET scans in both resting and hypercapnic conditions to obtain full quantification of rCBF and rCMR in the same subjects. Our aims were to determine (1) whether the patient sample was characterized by a consistent pattern of abnormality, either globally (whole brain) or regionally, (2) whether abnormalities were consistent or different across both rCBF and rCMR measurements, and (3) whether abnormalities would be accentuated by the hypercapnic challenge, a procedure designed to increase cerebral blood flow and highlight areas of inadequate vascular reserve. A consistent pattern of deficits across both blood flow and metabolic measurements would suggest a primary dysfunction in metabolism, given the usual close coupling of metabolism to flow. If deficits occurred primarily during rCBF measurement or were significantly accentuated during hypercapnia, the dysfunction would be considered largely vascular in origin.

METHODS

PARTICIPANTS

A sample of 35 patients and 17 controls participated in functional brain imaging assessments prior to a placebo-controlled clinical trial of the efficacy of intravenous ceftriaxone in patients. The patients historically met Center for Disease Control clinical and laboratory criteria for Lyme disease,[14] had a currently reactive IgG Western blot, prior treatment including at least 3 weeks of intravenous cephalosporin, and memory impairment. Memory impairment was defined by a demographically adjusted standardized T score on at least 1 index of the Wechsler Memory Scale that was 1 or less SD below the population mean (T score $\leq$40).[15] Patients were excluded who had a non–Lyme disease–related medical or neurological condition that could explain the memory impairment. On the basis of interviews using the Structured Clinical Interview for Diagnosis[16] and applying *DSM-IV* criteria,[17] patients were excluded if they currently or historically had any psychotic disorder. Patients with other current psychiatric disorders were excluded if onset of the disorder preceded the onset of Lyme disease. Controls had negative enzyme-linked immunosorbent and Western blot assays for Lyme disease and no evidence of memory impairment, a neurologic disorder, or a current axis 1 psychiatric disorder. The patient and control samples were matched on the mean, variance, and shape of distributions of age and education and the distribution of sex.

Prior to baseline assessment, patients and controls were withdrawn or refrained from all CNS-active medication and alcohol intake for at least 14 days, with the exception of medication for sleep such as lorazepam or zolpidem, for which the period was at least 7 days. Fluoxetine had to be discontinued at least 6 weeks prior to the baseline assessment. The afternoon before the PET and MRI procedures, patients and controls were admitted to the General Clinical Research Unit at the Columbia University Medical Center. Their diet was caffeine-free from admission until completion of the evaluations. Subjects did not smoke during the 12 hours prior to PET assessment.

All participants provided written informed consent, and the study was approved by the institutional review boards of the New York State Psychiatric Institute and Columbia University.

ASSESSMENT PROCEDURES

In addition to the imaging procedures, patients and controls underwent extensive cognitive, neurologic, rheumatologic, and psychiatric examinations. The cognitive assessments sampled 6 domains: attention (Stroop task; Continuous Performance Test), memory (Buschke Selective Reminding Test [verbal memory]; Benton Visual Retention Test [visual memory]), motor function (simple reaction time; choice reaction time; finger tapping), working memory (N-Back Test; A, Not B Logical Reasoning Test), psychomotor function (Trail Making A&B; Digit Symbol), and verbal fluency (Controlled Oral Word Association Test; Category Fluency Test). These measures are described elsewhere.[18,19] Using either published norms or a reference sample of healthy controls, scores on these tests were *z*-transformed and adjusted for the effects of sex, age, and education. Each domain score represented the average of the *z* scores for the primary tests within that cognitive domain. Overall performance was characterized by averaging the 6 domain scores to produce a cognitive index score. The neurological examination, which assessed 5 areas (sensory, motor, cranial nerves, reflexes, and associated motor [cerebellar and basal ganglia] functions) resulted in a summary score (range, 0-5) reflecting the number of areas with at least 1 minor or major abnormal finding. The rheumatologic examination assessed the number of joints in pain either at rest or while in motion. Participants also completed the Beck Depression Inventory-II (BDI-II),[20] Zung Anxiety Scale,[21] Symptom Checklist–90,[22] Fatigue Severity Scale,[23] McGill Pain Scale,[24] and Medical Outcomes Study Short Form–36[25] after the medication-free period. On the basis of a

medical history, a cardiovascular disease (CVD) risk factor score was derived following the procedures recommended by the American Heart Association.[26]

IMAGING PROCEDURES

Oxygen 15 PET

The $H_2{}^{15}O$ and 2-deoxy-2-(^{18}F)-D-glucose (FDG) (radioactively labeled water and glucose, respectively) were synthesized in a CTI computer-controlled chemistry process control unit (CTI Inc, Knoxville, Tennessee). Scans were performed with the Siemens ECAT EXACT HR+ (New York, New York). A 20-gauge Teflon catheter was inserted into the radial artery after examining for adequate collateral perfusion. The patient was then positioned in a fixed head-holding device and a 15-minute transmission scan was collected. Each rCBF measurement consisted of a bolus injection of 12 to 15 mCi of $H_2{}^{15}O$, followed by a 10-mL saline flush. After tracer arrival in the brain, a count-triggered 90-second emission scan (composed of three 30-second frames) was obtained in 3-dimensional mode. Arterial blood was withdrawn at a constant rate via an automated peristaltic pump and radioactivity was recorded. The scans were reconstructed using standard back-projection, filtering, and measured attenuation. Quantification of CBF (in milliliters per minute per 100 g) followed the autoradiographic technique.[27] For both CBF and CMR, absolute quantification was obtained by submitting the time-activity curves to the algorithms of the commercial PMOD software program (PMOD Technologies Ltd, Zurich, Switzerland). There was a 15-minute interval between serial injections.

Functional imaging scans commenced at the same time of day for all participants (9:30 AM). Urine for toxicology was obtained earlier that morning. Admission to the General Clinical Research Unit the previous afternoon ensured dietary control. The first oxygen 15 (^{15}O) scan was during an eyes-open, ears-unoccluded, resting condition (rest: room air). The only auditory stimulation was the background machine noise. Resting instructions were given 3 minutes before injection. This measurement was followed by a second resting assessment also under room air conditions, but with a mouth snorkel in place (rest: snorkel). This condition functioned as a control both for the first rest: room air assessment (same air) and for the hypercapnic challenge (same breathing apparatus). The third assessment involved hypercapnic challenge. Participants breathed 5% carbon dioxide (CO_2) mixed in the air from a tank through the snorkel. The CO_2 mixture was administered for 3 minutes prior to the ^{15}O injection and continued throughout the scan. For each ^{15}O scan, arterial blood sampling for Pa_{CO_2} was obtained prior to and following the assessment. Peak values were used to characterize the blood gas level during the measurement. Inhalation of CO_2 was chosen over administration of acetazolamide, given the more rapid onset and reversibility of hypercapnic effects with CO_2, the utility of Pa_{CO_2} monitoring, and uncertainty about the mechanisms of acetazolamide.[28] The FDG scan was performed after the 3 rCBF measurements.

FDG Positron Emission Tomography

The CMR for glucose was assessed during an eyes-open resting condition, with instructions for rest given 3 minutes prior to injection of 5 mCi of FDG. Forty minutes were allowed for uptake and equilibration, followed by a 60-minute PET scan composed of twelve 5-minute frames (3-dimensional acquisition). Arterial samples were repeatedly drawn by pump to derive a time-activity curve and to verify that blood glucose was stable. The scanning procedure resulted in greater than 60 million total counts. Each frame was reconstructed with standard filtered back-projection routines to a resolution of approximately 7 mm full width half maximum. Measured attenuation factors were used for all reconstructions. The frames were mathematically aligned and summed. For FDG, quantification was performed using the Sokoloff autoradiographic method as modified by Phelps.[29]

Magnetic Resonance Imaging

Magnetic resonance images were acquired using a dedicated 1.5-T GE Signa Advantage system (Chalfont St Giles, England). The PET and MRI data were coregistered to the T1-weighted spoiled gradient recalled images.[30] Results of the MRI analyses will be reported in a separate article.

STATISTICAL ANALYSIS

Analytic Strategy

Except where otherwise indicated, the patient and control groups were compared using analyses of covariance (ANCOVAs), with diagnostic group (patient vs control) as the between-subject factor and the 3 matching variables age, sex, and education as covariates. When significant effects of diagnostic group were obtained, the American Health Association (AHA) CVD risk factor score was added as an additional covariate to examine whether effects persisted once controlling for this factor. To explore whether differences in rates of current depressive disorder or severity of depressive symptoms were responsible for the between-group differences, additional secondary analyses were performed. One set excluded those patients who met *DSM-IV* criteria (n=8) for a current episode of any depressive disorder from the comparisons of the patient and control groups. Another set of secondary analyses added the BDI score to the standard set of covariates to determine whether the between-group differences persisted after controlling for the severity of depressive symptoms. All tests were 2-tailed and $\alpha = .05$ was used to determine statistical significance.

Global Effects

For each individual, the functional images were warped into a common probabilistic space. This routine coregistered the PET images to an MRI template derived from the structural images of an independent sample of control participants. The voxels in the probabilistic space had previously been identified as representing gray or white matter using an automated segmentation algorithm, and average CBF and CMR values were calculated for these tissue types. The ANCOVAs were conducted comparing the Lyme disease and control groups in global gray matter CBF and CMR values.

Distribution of Topographic Differences

Previous imaging studies have suggested that patients with Lyme disease show scattered abnormalities in CBF or CMR that may appear in gray or white matter and for which location may not be consistent across individuals. Marked but topographically inconsistent deficits would be missed by standard analytic paradigms, and we developed a new approach to address this issue.

All of the PET images were carefully checked for scan artifacts and were motion corrected. The images were registered to Montreal Neurological Institute space as implemented by Statistical Parametric Mapping (SPM99; Wellcome Trust Center for Neuroimaging at University College of London, London,

Table 1. Demographic and Clinical Features of the Samples

Variable[a]	Mean (SD)		*P* Value
	Patients With Lyme Disease (n=35)	Controls (n=17)	
Age, y	44.9 (12.9)	44.9 (11.3)	.99
Female, %	57.1	76.5	.17
Education, y	14.7 (2.6)	15.8 (2.3)	.16
AHA CVD score	3.0 (2.5)	2.1 (1.9)	.24
Duration of prior IV antibiotics, mo	2.1 (1.6)		
Duration of prior oral antibiotics, mo	7.0 (9.4)		
Duration of illness, mo	101.9 (75.0)		
Current pain, McGill Visual Analog Scale	4.9 (3.3)	0.1 (0.2)	<.001
Fatigue severity scale	5.3 (1.4)	2.0 (0.5)	<.001
Physical components scale, SF-36	36.2 (8.3)	55.9 (3.7)	<.001
Mental components scale, SF-36	40.8 (11.4)	56.3 (3.0)	<.001
Beck Depression Inventory	11.9 (8.2)	2.0 (2.4)	<.001
Zung Anxiety Index	47.5 (10.8)	32.9 (6.9)	<.001
DSM-IV current depressive episode, No.	8	0	.04
Joints in pain at rheumatologic examination, No.	5.9 (5.5)	0.6 (0.7)	<.001
Neurological examination summary score	2.3 (1.4)	0.7 (1.0)	<.001
Neurocognitive status			
Motor	−0.21 (1.29)	0.59 (0.65)	.005
Psychomotor	−0.17 (0.71)	0.94 (0.75)	<.001
Attention	−0.07 (0.96)	0.26 (0.78)	.19
Memory	−0.65 (1.02)	0.52 (0.40)	<.001
Working memory	−0.63 (1.00)	0.29 (0.68)	<.001
Language	−0.75 (0.80)	0.47 (0.68)	<.001
Overall index score	−0.42 (0.62)	0.51 (0.38)	<.001

Abbreviations: AHA, American Heart Association; CVD, cerebrovascular disease; IV, intravenous; SF-36, Medical Outcomes Study Short Form-36.

England).[31] The image intensity values of the controls at each voxel were normalized so the mean at each voxel was 0 and the standard deviation was 1. The distributions in the control group were then imposed on the patient group using a standard *z* transformation. Thus, the globally normalized CBF or FDG *z* statistic at each voxel reflected the extent of the difference from average in the control sample in units of standard deviation. For each individual, the number of voxels were counted that represented varying degrees of departure above or below the average values for controls. In this way, the groups could be compared in overall number of voxels with extreme values regardless of location.

Traditional Topographic Analyses

The SPM99 software was used to examine differences between the patient and control groups in the topography of rCBF and rCMR values. A Gaussian kernel of 11 mm full width half maximum for ^{15}O images and 7 mm full width half maximum for FDG images was applied to spatially smooth the images. Images of raw counts were used instead of quantified data and normalized to the scan mean. The global mean across voxels was proportionally scaled to 50 and the analysis threshold, applied to normalized data, was set to a 0.8 proportion of the global mean. The overall height threshold for identifying potentially significant clusters was set to $P \leq .01$, with an extent threshold of 25 voxels. A *z* value of 3.0 or greater was required for considering a cluster significant. As before, age, sex, and education level served as covariates in all between-group analyses. These thresholds reflected a conservative choice in identifying areas of between-group significant difference. The availability of 2 resting rCBF measurements, an rCBF measurement under hypercapnia, and a measurement of rCMR allowed for determination of the reliability of the rCBF resting deficits, their expression during hypercapnia, and coupling with metabolic abnormalities.

RESULTS

At baseline, the patient and control groups did not differ in the matching variables, age, sex, and education level (**Table 1**). Nonetheless, the patient group reported more severe pain and fatigue and greater impairment in physical function, performed worse on neurocognitive testing, and, on examination, had more joints with pain and more areas of neurologic abnormality. They also reported greater severity of depression and anxiety and, by *DSM-IV* diagnosis, presented with a higher rate of having a current episode of a depressive disorder.

GLOBAL CMR AND CBF AT REST

The groups did not differ in estimates of resting global CMR (**Table 2**) while controlling for age, sex, and education level ($F_{1,39}=0.45$; $P=.65$). The patient group had significantly higher whole-brain CBF than the control group in the initial resting condition ($F_{1,40}=7.28$; $P=.01$), but not in the subsequent snorkel ($F_{1,34}=2.58$; $P=.12$) or hypercapnic ($F_{1,28}=0.09$; $P=.77$) conditions. This same pattern held when the whole-brain voxels were segmented into gray and white matter tissue types and when the CVD risk factor score was added as a covariate (data not shown).

The higher global CBF values in patients during the first room air resting measurement may have reflected a

Table 2. Brain Imaging Global Values

Variable	Mean (SD)		*P* Value
	Patients With Lyme Disease	Controls	
Total sample			
CMR, resting (n=31, 13)	3.25 (1.91)	3.83 (2.30)	.65
CBF, resting: room air (n=31, 14)	45.51 (5.85)	38.77 (11.69)	.01
CBF, resting: snorkel with room air (n=28, 11)	41.61 (6.92)	40.34 (13.81)	.12
CBF, hypercapnia (n=24, 9)	45.06 (6.60)	45.83 (9.22)	.76
Subsample of patients who had hypercapnia			
CMR, resting (n=23, 8)	2.88 (1.83)	3.58 (1.81)	.41
CBF, resting: room air (n=23, 9)	45.69 (6.43)	37.64 (13.67)	.02
CBF, resting: snorkel with room air (n=23, 7)	41.81 (7.35)	38.62 (14.83)	.05
CBF, hypercapnia (n=24, 9)	45.06 (6.60)	45.83 (9.22)	.76

Abbreviations: CBF, cerebral blood flow in units of milliliters per minute per 100 g; CMR, cerebral metabolic rate in units of milligrams per minute per 100 g.

"first run" effect. When comparing global CBF during the first room air and the subsequent snorkel condition, the patient group showed a significant decrease (t_{26}=2.79; $P<.01$), while the control group had no change (t_{10}=–0.26; $P=.80$). During a secondary analysis, when the patients with a current diagnosis of a depressive disorder (n=8) were excluded, the between-group difference in global CBF during the first resting measurement was no longer significant ($F_{1,32}$=1.75; $P=.19$). When BDI scores were added as a covariate, the patterns in Table 2 were essentially unaltered.

GLOBAL CBF AND HYPERCAPNIC REACTIVITY

The patient group showed diminished hypercapnic reactivity when the first resting measurement was used as the baseline. The 23 patients who had fully quantified resting and hypercapnic measurements had a mean (SD) decrease of 3.82% (14.21%), while 9 controls showed an increase of 32.31% (45.58%) ($F_{1,27}$=7.27; $P=.01$). However, as noted earlier, CBF in patients was elevated at the first compared with the second measurement. Nonetheless, when the second measurement (snorkel condition) was used as the baseline, the 23 patients continued to show diminished hypercapnic reactivity (mean [SD], 8.28% [15.84%]) compared with 7 controls (mean [SD], 28.12% [35.36%]; $F_{1,25}$=6.47; $P<.02$).

The diminished hypercapnic reactivity in the patient sample could not be attributed to differences in CO_2 inhalation, as reflected in blood gas values. The 2 groups did not differ in peak $PaCO_2$ values during any of the 3 measurements, nor in the percentage of change in these values during hypercapnia relative to the 2 earlier measurements (all $P>.09$). The diminished reactivity in the patient sample remained significant (both $P<.01$) when the percentage of change in $PaCO_2$ was added as a covariate to the ANCOVAs on the percentage of change in CBF during hypercapnia relative to either of the preceding resting measurements. Excluding patients with a current diagnosis of a depressive disorder or adding BDI or AHA CVD scores as a covariate did not alter these patterns.

DISTRIBUTION OF EXTREME VALUES

The patient and control groups did not differ in repeated measures ANOVA on the distribution of CMR *z* scores for gray matter voxels (**Figure 1**) ($F_{2.08,93.57}$=1.21; $P=.30$). Although the distribution for patients was shifted slightly to the left, suggesting a larger number of voxels with reduced CMR, this analysis indicated that, independent of topography, there was not an excess of voxels with low or high CMR in either group across all brain regions. The same pattern occurred in all of the CBF analyses (Figure 1), none of which yielded an interaction between diagnostic group and *z* score bin (all $P\geq.18$). In contrast, the *z* bin analyses consistently yielded significant effects of age, sex, and education level ($P<.05$). Whole-brain *z* bin distributions were also consistently found to be a function of the CVD risk factor score when this score was added as an additional covariate ($P<.05$).

TOPOGRAPHIC ANALYSES

FDG Rest

Based on a sample of 33 patients and 17 controls, 12 clusters involving 3049 voxels were identified in the SPM covariance analysis with patients having lower FDG than controls (**Table 3**; **Figure 2**). There were 3 clusters, involving 680 voxels, where CMR was higher in patients than in controls. The FDG regional pattern had notable similarity to the group differences in CBF (see below). Across the CMR and CBF analyses, there were widely distributed reductions in left prefrontal and bilateral posterior gray and white matter areas. The largest clusters of reduced CMR in patients were located in the left temporal and frontal areas as well as the right cingulate. Notably, there was little evidence of CMR reduction in patients in the right prefrontal cortex; this was mirrored in the CBF analyses. Of the 3 clusters showing increased CMR in patients, the ones in the right occipital lingual gyrus and the right frontal gyrus were also seen in the CBF conditions (Figure 2). Contrary to the CBF analyses, a relative CMR increase was also observed in patients in the left insula. In addition to the main effects

of diagnostic group, there were marked main effects of each of the covariates on CMR. Excluding patients with a current diagnosis of a depressive disorder or adding BDI or AHA CVD scores as a covariate did not alter these patterns. Lower CMR in widespread regions was associated with advanced age (9 clusters, 19 539 voxels), male sex (19 clusters, 5649 voxels), and fewer years of education (11 clusters, 2103 voxels). There were few significant clusters opposite in direction.

CBF Rest: Room Air Condition

The SPM covariance analysis contrasting patients (n=35) and controls (n=17) yielded 9 clusters involving 2828 voxels, where CBF was greater in controls than in patients (Table 3; Figure 2). Patients had higher CBF than the control group in only 1 cluster, involving 222 voxels. The CBF reductions in patients pertained to both cortical gray matter structures and underlying white matter and were mainly distributed in left frontal (Brodmann area [BA] 10) and bilateral temporal and occipital regions. In particular, the right prefrontal cortex appeared to be spared or elevated in the patients with Lyme disease, while bilateral posterior and left parahippocampal areas were most affected. The 1 area of increased CBF in patients relative to controls was in the right medial frontal gyrus (BA 10).

CBF Rest: Snorkel Condition

Data were available for 29 patients and 14 controls. An SPM subtraction analysis was conducted contrasting CBF profiles in the resting snorkel and preceding resting room air conditions. A highly circumscribed pattern was observed across and within the diagnostic groups. Cerebral blood flow was markedly higher in the snorkel condition in the left and right sensorimotor cortices. There were no CBF increases in the room air relative to the snorkel condition. This indicated that the principal effect of the snorkel condition was to increase CBF in primary sensorimotor areas, presumably reflecting stimulation of the mouth. Effectively, with this difference aside, the snorkel condition could be considered a second resting measurement.

To determine whether the pattern of baseline topographic abnormalities was consistently observed across the measurement conditions, an SPM analysis was conducted contrasting patients and controls, restricting the data to the snorkel condition. There were 9 clusters involving 2363 voxels in which patients had lower CBF than controls (Table 3). Inspection of Figure 2 suggested that the pattern of CBF abnormality in patients was similar in the snorkel and room air conditions. There were only 2 significant clusters, involving 240 voxels, in the opposite direction.

CBF Hypercapnia

Data from the hypercapnic manipulation were available for 24 patients and 10 controls. As in the analysis of the snorkel condition, there was a marked bilateral increase in sensorimotor cortex when the hypercapnic and first resting room air condition were contrasted, with no change in topography when the hypercapnic and snorkel conditions were compared. Thus, relative to the first room air condition, the major topographic change in the 2 subsequent conditions reflected activation of the sensorimotor cortex, presumably due to motor and sensory effects involved in use of the snorkel.

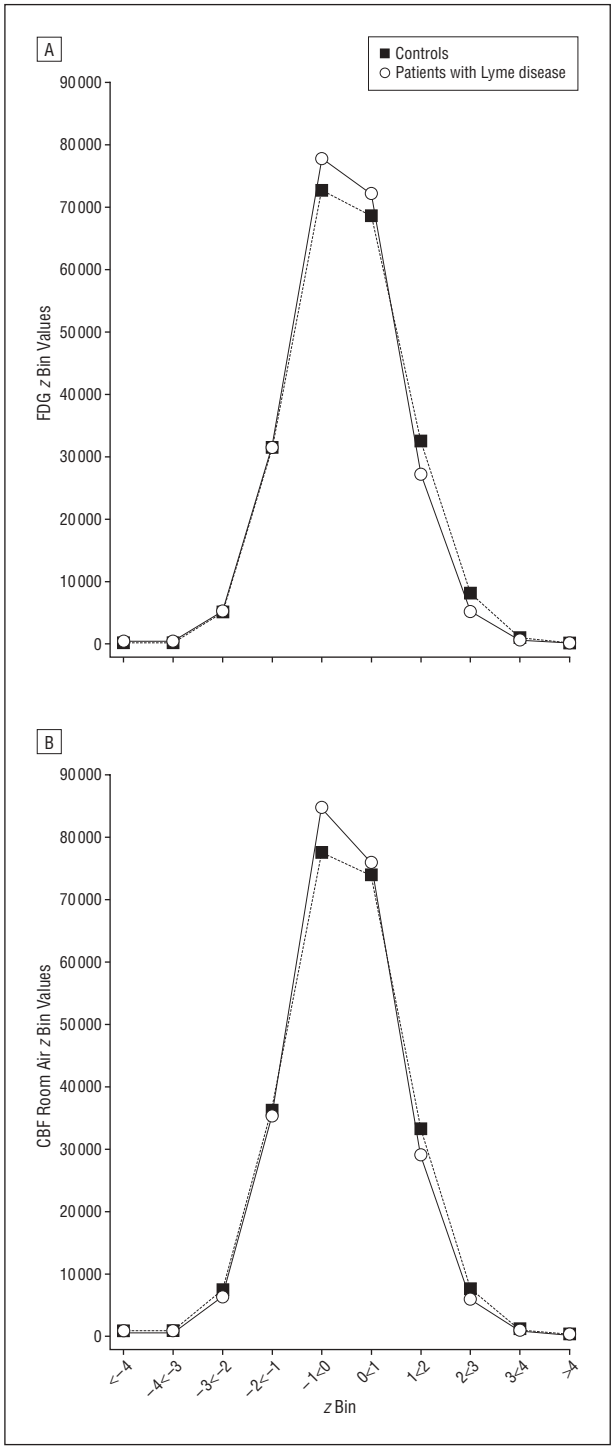

Figure 1. Distribution of voxels by *z* bin scores in patients with Lyme disease and healthy volunteers (controls). Distribution is for measurement of cerebral metabolic rate for glucose (A) and for the first resting (room air) measurement of cerebral blood flow (CBF) (B). The *z* bins were determined by the distribution of values for gray matter in the control sample. While the patient group is shifted slightly to the left of the controls, there were no significant differences between the groups in *z* bin distributions for any assessment. FDG indicates 2-deoxy-2-(^{18}F)-D-glucose.

Table 3. Clusters in Which Patients With Lyme Disease Differed From Controls in CMR or CBF[a]

	MNI Coordinates			Voxel, No.	*z* Score
	x	*y*	*z*		
CMR rest, > patients					
Left temporal, superior temporal gyrus, WM (GM, BA 22, distance=3)	−54	−50	24	531	4.07
Right parietal, inferior parietal lobule, WM (GM, BA 40, distance=3)	56	−40	32	265	3.51
Left temporal, middle temporal gyrus, WM (GM, BA 39, distance=2)	−46	−70	32	334	3.43
Left frontal, superior frontal gyrus, WM (GM, BA 8, distance=2)	−18	46	46	62	3.41
Left sublobar, extranuclear, WM (GM, claustrum, distance=2)	−34	22	−2	439	3.40
Right limbic, posterior cingulate, GM, BA 30	24	−64	16	178	3.35
Left frontal, subgyral, WM (GM, BA 6, distance=3)	−34	−8	46	527	3.30
Right sublobar, insula, GM, BA 13	52	4	−2	154	3.21
Left parietal, precuneus, GM, BA 7	−12	−54	72	36	3.07
Right limbic, cingulate gyrus, GM, BA 24	4	8	44	309	3.03
Left cerebellum, anterior lobe, fastigium, GM	−6	−48	−22	75	3.02
Left parietal, posterior central gyrus, WM	−58	−14	22	139	3.01
CMR rest, patients > controls					
Left sublobar, extranuclear, WM (GM, BA 13, distance=1)	−36	−6	26	172	4.08
Right occipital, lingual gyrus, WM (GM, BA 18, distance=3)	14	−82	2	316	3.29
Right frontal, superior frontal gyrus, WM (GM, BA 9, distance=4)	20	52	18	192	3.14
CBF room air, controls > patients					
Left temporal, supramarginal gyrus, WM (GM, BA 39, distance=1)	−60	−52	32	149	3.61
Right occipital, middle occipital gyrus, WM (GM, BA 19, distance=2)	42	−86	24	155	3.54
Left frontal, superior frontal gyrus, GM, BA 10	−12	70	8	123	3.45
Left occipital, subgyral, WM (fusiform, GM, BA 37, distance=2)	−48	−58	−6	525	3.43
Right temporal, superior temporal gyrus, GM, BA 22	58	−6	2	556	3.40
Left limbic, parahippocampal gyrus, WM (GM, BA 36, distance=1)	−40	−26	−14	883	3.32
Right limbic, posterior cingulate (GM, BA 31, distance=3)	20	−66	20	212	3.29
Right middle occipital gyrus, (GM, BA 19, distance=2)	58	−74	8	126	3.19
Left midoccipital gyrus, WM (limbic, posterior cingulate, GM, BA 30, distance=4)	−32	−70	24	99	3.08
CBF room air, patients > controls					
Right frontal, medial frontal gyrus, WM (GM, BA 10, distance=2)	18	52	2	222	3.05
CBF snorkel, controls > patients					
Left parietal, postcentral gyrus, WM (GM, BA 40, distance=1)	−66	−18	22	367	4.10
Right temporal, superior temporal gyrus, GM, BA 22	52	−14	0	646	3.66
Left limbic, cingulate gyrus (GM, BA 24, distance=1)	−2	−2	42	335	3.45
Right frontal, middle frontal gyrus, GM, BA 9	50	28	36	114	3.29
Left frontal, superior frontal gyrus, WM (GM, BA 8, distance=1)	−18	40	52	77	3.29
Left cerebellum anterior lobe, culmen, GM	−40	−54	−22	569	3.24
Right frontal, middle frontal gyrus, WM (GM, BA 47, distance=2)	56	44	−10	92	3.20
Left frontal, subgyral, WM (limbic, cingulate gyrus, GM, BA 31, distance=4)	−22	−20	40	90	3.03
Right temporal, transverse temporal gyrus, WM (GM, BA 41, distance=2)	42	−30	14	73	3.03
CBF snorkel, patients > controls					
Right occipital, lingual gyrus, GM, BA 18	12	−80	−4	167	3.50
Right frontal, subgyral, WM (limbic, anterior cingulate, GM, BA 32, distance=3)	−18	−34	2	73	3.18
CBF hypercapnia, controls > patients					
Right cerebellum, posterior lobe, declive, GM	54	−74	−20	393	4.85
Left limbic, parahippocampal gyrus, WM (GM, BA 36, distance=2)	−38	−28	−12	539	3.91
Left limbic, posterior cingulate, WM (GM, BA 30, distance=3)	−10	−48	22	245	3.83
Left frontal, middle frontal gyrus, GM, BA 6	−40	−4	52	1086	3.80
Left parietal, precuneus WM (superior parietal GM, BA 7, distance=4)	−24	−54	48	1132	3.74
Right sublobar, extranuclear WM (insula, GM, BA 13, distance=3)	42	−24	8	1515	3.59
Left occipital, cuneus, GM, BA 19	−24	−90	34	171	3.56
Left temporal, fusiform gyrus, GM, BA 37	−58	−62	−12	814	3.55
Right frontal, middle frontal gyrus, GM, BA 6	34	4	52	750	3.53
Left parietal, superior parietal lobule, GM, BA 7	−4	−64	70	189	3.44
Left parietal, postcentral gyrus, GM, BA 40	−66	−22	22	115	3.43
Left limbic, cingulate gyrus, WM (GM, BA 23, distance=2)	−6	−6	36	812	3.30
Right temporal, subgyral WM (superior temporal gyrus, GM, BA 13, distance=4)	50	−46	32	545	3.26
Right limbic lobe, posterior cingulate, GM, BA 30	22	−64	44	209	3.19
Left inferior parietal lobule, WM (posterior central gyrus, GM, BA 5, distance=2)	−40	−42	66	74	3.05
CBF hypercapnia, patients > controls					
Right medial frontal gyrus, WM (superior frontal gyrus, GM, BA 10, distance=1)	20	58	−6	224	3.46

Abbreviations: BA, Brodmann area; CBF, cerebral blood flow; CMR, cerebral metabolic rate; GM, gray matter; MNI, Montreal Neurological Institute; WM, white matter.
[a] Nearest GM is marked in parentheses next to the WM along with the distance in millimeters and Brodmann area.

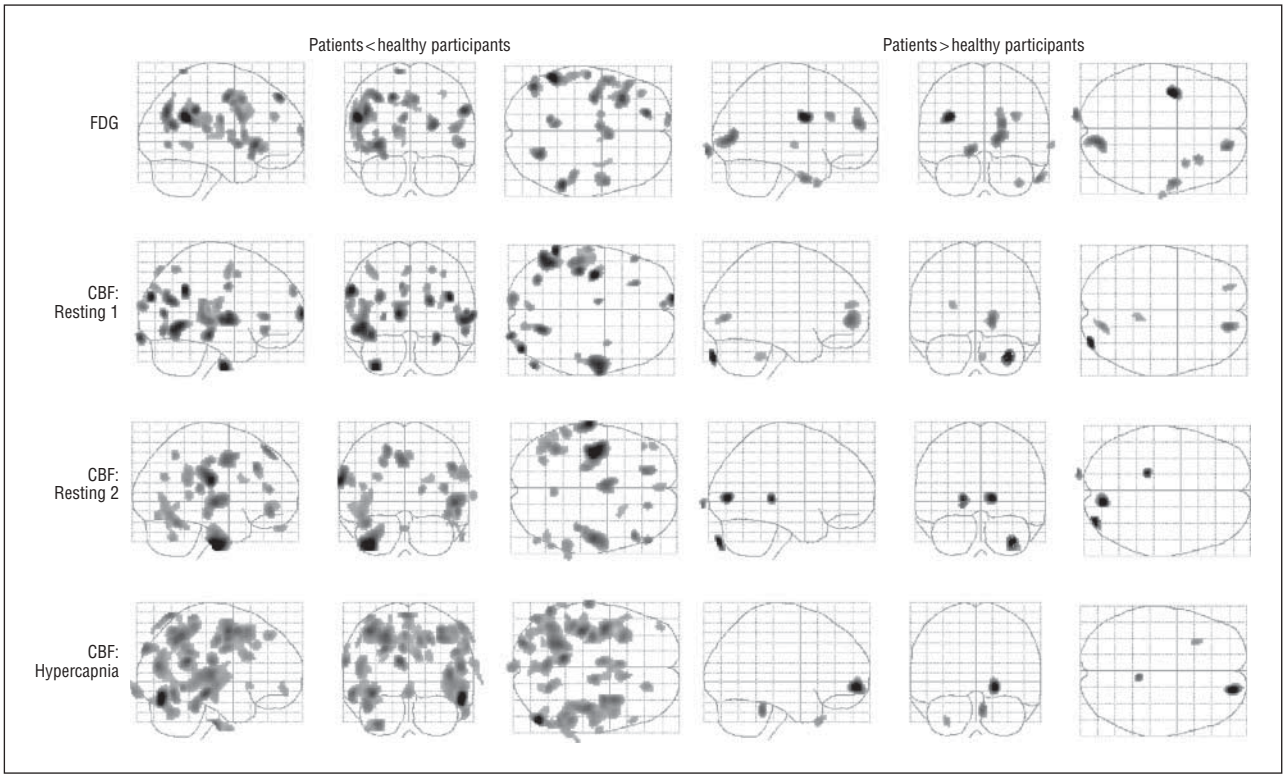

Figure 2. Statistical Parametric Mapping images of cerebral brain metabolism and blood flow (CBF) under 3 conditions: resting 1 indicates room air; resting 2, room air with snorkel; hypercapnia, room air enhanced with carbon dioxide with snorkel. Patients have multiple areas of decreased metabolism and blood flow that, for the flow, are enhanced under hypercapnia. There are very few areas where patients had increased metabolism or flow compared with the controls. FDG indicates 2-deoxy-2-(^{18}F)-D-glucose.

When the SPM analysis was conducted solely on the data from the hypercapnic condition, there were 15 clusters involving 8589 voxels in which patients had lower CBF than controls. The pattern of CBF abnormality in patients was amplified relative to either of the prior resting measurements. Inspection of Figure 2 suggested that the abnormalities observed under the resting conditions were expressed more widely with the hypercapnic manipulation as opposed to involving a new pattern of deficits. There was only 1 significant cluster in the opposite direction, involving 224 voxels, with patients showing higher relative CBF in the right superior frontal gyrus gray matter.

CBF Analyses: Covariates

As in the CMR analysis, each SPM analysis contrasting the patient and control groups in the 3 CBF conditions used age, sex, and education as covariates. Each of these analyses yielded marked effects for each covariate. For example, in the first resting measurement, advanced age (10 clusters, 18 492 voxels), male sex (19 clusters,14 655 voxels), and fewer years of education (8 clusters, 2922 voxels) were each associated with widely distributed CBF reductions. There were few significant effects in the opposite direction. These effects were also highly consistent with the CMR findings. The between-group differences observed in each of the CBF conditions were essentially unaltered when excluding patients with a current diagnosis of a depressive disorder or adding the BDI or AHA CVD score as an additional covariate.

COMMENT

This study examined the differences in CBF and CMR between demographically matched controls and patients with objective cognitive abnormalities who had a well-documented history of Lyme disease that had been previously treated with at least 3 weeks of intravenous antibiotic therapy. These patients reported that their cognitive symptoms emerged after contracting Lyme disease and that their symptoms either returned or persisted despite prior treatment. Prior reports had suggested that patients with later-stage Lyme disease have patchy hypoperfusion in the CNS that is similar to what one would see in a condition resulting in CNS vasculitis.[10,32] This patchy hypoperfusion could reflect either a true vasculitic process or an alteration in vascular demand as a result of diffuse and scattered metabolic deficits.

The SPM analyses revealed that, compared with controls, the patients had substantial differences in specific brain regions of blood flow and metabolism. There were only a few areas involving a relatively small number of voxels in which patients showed higher CBF or CMR than controls—specifically, the right frontal gyrus (BA 9 and BA 10). On the other hand, many areas showed lower CBF and CMR in the patient group—specifically, bilateral gray and white matter in temporal, parietal and limbic regions and the left frontal cortex (Table 3; Figure 2). These findings are congruent with prior articles that described hypofunction, particularly in the temporal area, in patients with Lyme disease.[11-13] Notably in this study, deficits were rare in the

right frontal cortex. Many of the areas of abnormal CBF and CMR identified in Table 3 have been associated with symptom complexes common to patients with Lyme encephalopathy including problems with language fluency (BA 22, 39, and 40), executive functioning and working memory (BA 9 and 10), memory encoding and retrieval (BA 10, 30, and 36), visual attention (BA 19), spatial orientation (BA 7), emotional processing of pain (BA 13), and regulation of autonomic function and rational cognition (BA 24).

Compared with controls, the patients with Lyme encephalopathy did not have a randomly scattered excess of either extreme hyperfunction or hypofunction in either cerebral blood flow or metabolic rate. Although the analytic method we developed was sensitive to demographic factors such as age and sex that diffusely affect CBF and/or CMR, there was no evidence in this study that the patient group was characterized by an excess of extreme values.

These findings suggest that a distributed network or set of networks is abnormal in individuals who have persistent symptoms after conventional treatment of Lyme disease. Rather than a randomly scattered distribution of heterogeneous hypoperfusion that varies significantly from person to person, the deficits were sufficiently large and consistent in the patient group for SPM to reveal multiple regions where patients had lower CBF and CMR and a much smaller set of deficits where patient CBF and CMR exceeded controls. Furthermore, the consistency of these deficits across 4 measures of brain function (1 CMR and 3 CBF) supports the reliability of the findings and the notion that a uniform disease process was responsible for the abnormalities.

There was little evidence in this study to suggest that patients had a global deficit in resting blood flow or metabolism. Although the first resting room air CBF measurement revealed a global increase in the patient sample, this difference did not persist through the second resting room air: snorkel measurement. Higher global functional activity is often seen in a first resting measurement relative to subsequent measurements and has usually been attributed to the greater emotional reactivity with the initial measurement.[33,34] Supporting the hypothesis that measurement anxiety may have accounted for the higher CBF seen at the first but not the second measurement was the observation that an elevated measurement during the first resting procedure was no longer noted when the 8 patients with a comorbid depressive disorder were excluded.

When either the first or second resting CBF condition was used as a baseline to assess the CBF response to the hypercapnic challenge, the patients showed diminished vasodilation relative to the control group. Diminished vasodilation may occur because perfusion pressure is already maximal or because the vasculature is otherwise compromised. Some of the dysfunction in neurologic Lyme disease may result from inflammatory changes in CNS blood vessels—a hypothesis supported by case reports of diffuse or focal vasculitides and strokes[35-37] attributed to Lyme disease and by perivascular inflammation noted in brain biopsies of patients with Lyme disease.[38] However, while the results suggest that a vascular disease process was active in the patient sample, the patients and controls did not differ in global CBF during the hypercapnic assessment. The observation of a hypercapnic deficit in patients was likely owing to higher absolute global values in the patient groups in the 2 prior resting measurements, although this difference only achieved statistical significance for the first resting measurement. Furthermore, the deficits seen during hypercapnia, while broader and more extensive than those seen during any of the other CBF or CMR measurements, did not reflect a change in pattern as much as a widening of the boundaries of the areas of deficits observed in the other CBF and CBF assessments (Figure 2). These observations suggest that there was strong coupling between the CBF and CMR deficits and that the regional abnormalities observed in this study were primarily metabolically driven.

The few controlled MRI studies of posttreatment Lyme disease are consistent with the impression that the persistent brain effects are not primarily due to structural vascular disease. One MRI study[9] that used T1, T2, fluid-attenuated inversion recovery, and diffusion-weighted imaging sequences found no significant difference in the number of structural abnormalities in patients with posttreatment Lyme disease compared with age- and sex-matched controls and no relationship with the number of lesions and the duration of disease. A second MRI study[39] found no difference in the mean or peak magnetization transfer ratio between patients with posttreatment Lyme disease and controls, indicating that the multifocal perfusion deficits previously reported on SPECT imaging and now demonstrated with PET imaging are not associated with detectable structural damage.

This study does not address whether the imaging abnormalities reflected persistent *B burgdorferi* infection as opposed to a postinfectious process. We also cannot prove that the imaging abnormalities might not be accounted for by another unexamined variable in which the groups differed. For example, we examined whether depression might have accounted for the differences because it is well known that depression is associated with functional imaging abnormalities.[40-42] In this case, the functional imaging findings were unaltered when individuals with depressive comorbidity were removed from the patient sample or when scores on the BDI were used as a covariate. Similarly, the findings were unaltered after controlling for cerebrovascular disease risk factor scores. Finally, although patients reported developing cognitive problems only after getting Lyme disease, we cannot be certain that the identified brain regional abnormalities were not present prior to infection. The consistency of the regionally specific abnormalities in CBF and CMR, however, support the likelihood that the observed dysfunction reflects a unitary etiology that resulted in either sustained damage from prior infection with *B burgdorferi* or an ongoing CNS disease process.

The areas of prominently reduced metabolism and blood flow in our study were the temporal-parietal and limbic areas bilaterally as well as the left frontal cortex. The results of this study are congruent with clinical series that have described multifocal areas of hypofunction in both cortical and subcortical white matter, particularly in the temporal lobes.[11-13] Although helpful in confirming objective central nervous system abnormalities in a patient with a history of Lyme disease, this pattern of hypofunction is nonspecific and cannot be used to make the diagnosis of Lyme encephalopathy. Indeed, a pattern of multifocal cortical and subcortical hypofunction can occur from other causes as well, such as chronic cocaine use, human immunodeficiency virus infection, and systemic lupus erythematosus.

In conclusion, this study demonstrates that patients with persistent encephalopathy after treatment for Lyme disease have objective neurobiological dysfunction.

Submitted for Publication: May 28, 2008; final revision received August 16, 2008; accepted August 23, 2008.
Correspondence: Brian A. Fallon, MD, Department of Psychiatry, Lyme and Tick-Borne Diseases Research Center, Columbia University, 1051 Riverside Dr, Unit 69, New York, NY 10032 (baf1@columbia.edu).
Author Contributions: Drs Fallon and Sackeim (the principal and coprincipal investigators of the study, respectively) take responsibility for the integrity of the data and the accuracy of the data analysis. All authors had full access to the data.
Financial Disclosure: Dr Fallon reports directing the Lyme and Tick-Borne Diseases Research Center and has received grant funds from federal private nonprofit foundations to support this work.
Funding/Support: This study was supported in part by grant RO1 NS38636 from the National Institute of Neurological Disorders and Stroke, Bethesda, Maryland (Dr Fallon); grant R01 MH55646 to from the National Institute of Mental Health, Bethesda, Maryland (Dr Sackeim); the Columbia University Lyme and Tick-borne Diseases Research Center established by Time for Lyme, Inc, and the Lyme Disease Association; New York Psychiatric Insitute; and the Irving Institute for Clinical and Translational Research at Columbia University Medical Center.
Additional Contributions: We thank Megan Romano, BA, Tani Viera, BA, Dexterrie Clemente, MA, Marcia Kimmeldorf, MA, Paul Johnson, BA, and Tyler Tarabula, BA, for their work on this project.

REFERENCES

1. Shadick NA, Phillips CB, Sangha O, Logigian EL, Kaplan RF, Wright EA, Fossel AH, Fossel K, Berardi V, Lew RA, Liang MH. Musculoskeletal and neurologic outcomes in patients with previously treated Lyme disease. *Ann Intern Med*. 1999;131(12):919-926.
2. Cairns V, Godwin J. Post-Lyme borreliosis syndrome: a meta-analysis of reported symptoms. *Int J Epidemiol*. 2005;34(6):1340-1345.
3. Cameron D, Gaito A, Harris N, Bach G, Bellovin S, Bock K, Bock S, Burrascano J, Dickey C, Horowitz R, Phillips S, Meer-Scherrer L, Raxlen B, Sherr V, Smith H, Smith P, Stricker R; ILADS Working Group. Evidence-based guidelines for the management of Lyme disease. *Expert Rev Anti Infect Ther*. 2004;2(1)(suppl):S1-S13.
4. Feder HM Jr, Johnson B, O'Connell S, Shapiro ED, Steere AC, Wormser GP, Agger WA, Artsob H, Auwaerter P, Dumler JS, Bakken JS, Bockenstedt LK, Green J, Dattwyler RJ, Munoz J, Nadelman RB, Schwartz I, Draper T, McSweegan E, Halperin JJ, Klempner MS, Krause PJ, Mead P, Morshed M, Porwancher R, Radolf JD, Smith RP Jr, Sood S, Weinstein A, Wong SJ, Zemel L; Ad Hoc International Lyme Disease Group. A critical appraisal of "chronic Lyme disease" [correction published in *N Engl J Med*. 2008;358(10):1084]. *N Engl J Med*. 2007;357(14):1422-1430.
5. Alaedini A, Latov N. Antibodies against OspA epitopes of *Borrelia burgdorferi* cross-react with neural tissue. *J Neuroimmunol*. 2005;159(1-2):192-195.
6. Halperin JJ, Pass HL, Anand AK, Luft BJ, Volkman DJ, Dattwyler RJ. Nervous system abnormalities in Lyme disease. *Ann N Y Acad Sci*. 1988;539:24-34.
7. Krüger H, Heim E, Schuknecht B, Scholz S. Acute and chronic neuroborreliosis with and without CNS involvement: a clinical, MRI, and HLA study of 27 cases. *J Neurol*. 1991;238(5):271-280.
8. Halperin JJ, Luft BJ, Anand AK, Roque CT, Alvarez O, Volkman DJ, Dattwyler RJ. Lyme neuroborreliosis: central nervous system manifestations. *Neurology*. 1989;39(6):753-759.
9. Aalto A, Sjowall J, Davidsson L, Forsberg P, Smedby O. Brain magnetic resonance imaging does not contribute to the diagnosis of chronic neuroborreliosis. *Acta Radiol*. 2007;48(7):755-762.
10. Fallon BA, Das S, Plutchok JJ, Tager F, Liegner K, Van Heertum R. Functional brain imaging and neuropsychological testing in Lyme disease. *Clin Infect Dis*. 1997;25(suppl 1):S57-S63.
11. Logigian EL, Johnson KA, Kijewski MF, Kaplan RF, Becker JA, Jones KJ, Garada BM, Holman BL, Steere AC. Reversible cerebral hypoperfusion in Lyme encephalopathy. *Neurology*. 1997;49(6):1661-1670.
12. Fallon BA, Keilp J, Prohovnik I, Heertum RV, Mann JJ. Regional cerebral blood flow and cognitive deficits in chronic lyme disease. *J Neuropsychiatry Clin Neurosci*. 2003;15(3):326-332.
13. Newberg A, Hassan A, Alavi A. Cerebral metabolic changes associated with Lyme disease. *Nucl Med Commun*. 2002;23(8):773-777.
14. Centers for Disease Control and Prevention (CDC). Recommendations for test performance and interpretation from the Second National Conference on Serologic Diagnosis of Lyme Disease. *MMWR Morb Mortal Wkly Rep*. 1995;44(31):590-591.
15. Wechsler D. *Wechsler Memory Scale*. 3rd ed. San Antonio, TX: The Psychological Corporation; 1997.
16. Spitzer RL, Williams JBW, Gibbon M, First MB. *Structured Clinical Interview for DSM-III-R: SCID-P - Patient Edition*. Arlington, VA: American Psychiatric Press, Inc; 1990.
17. American Psychiatric Association. *Diagnostic and Statistical Manual of Mental Disorders*. 4th ed. Arlington, VA: American Psychiatric Publishing Inc; 2000.
18. Keilp JG, Sackeim HA, Mann JJ. Correlates of trait impulsiveness in performance measures and neuropsychological tests. *Psychiatry Res*. 2005;135(3):191-201.
19. Sackeim HA, Keilp JG, Rush AJ, George MS, Marangell LB, Dormer JS, Burt T, Lisanby SH, Husain M, Cullum CM, Oliver N, Zboyan H. The effects of vagus nerve stimulation on cognitive performance in patients with treatment-resistant depression. *Neuropsychiatry Neuropsychol Behav Neurol*. 2001;14(1):53-56.
20. Beck A, Steer RA, Brown GA. *Manual for the Beck Depression Inventory-II*. San Antonio, TX: Psychological Corporation; 1996.
21. Zung WW. A rating instrument for anxiety disorders. *Psychosomatics*. 1971;12(6):371-379.
22. Derogatis LR, Rickels K, Rock AF. The SCL-90 and the MMPI: a step in the validation of a new self-report scale. *Br J Psychiatry*. 1976;1:280-289.
23. Krupp LB, LaRocca NG, Muir-Nash J, Steinberg AD. The fatigue severity scale: application to patients with multiple sclerosis and systemic lupus erythematosus. *Arch Neurol*. 1989;46(10):1121-1123.
24. Melzack R. The short-form McGill Pain Questionnaire. *Pain*. 1987;30(2):191-197.
25. Ware JE, Kosinski M. *Physical and Mental Health Summary Scales: A User's Manual*. Boston, MA: The Health Institute; 1994.
26. Davis PH, Dambrosia JM, Schoenberg BS, Schoenberg DG, Pritchard DA, Lilenfeld AM, Whisnanat JP. Risk factors for ischemic stroke: a prospective study in Rochester, Minnesota. *Ann Neurol*. 1987;22(3):319-327.
27. Herscovitch P. Cerebral blood flow and metabolism measured with oxygen-15 radiotracers. *J Neuropsychiatry Clin Neurosci*. 1989;1(1):S19-S29.
28. Vorstrup S. Tomographic cerebral blood flow measurements in patients with ischemic cerebrovascular disease and evaluation of the vasodilatory capacity by the acetazolamide test. *Acta Neurol Scand Suppl*. 1988;114:1-48.
29. Phelps ME, Huang SC, Hoffman EJ, Selin C, Sokoloff L, Kuhl DE. Tomographic measurement of local cerebral glucose metabolic rate in humans with (F-18)2-fluoro-2-deoxy-D-glucose: validation of method. *Ann Neurol*. 1979;6(5):371-388.
30. Turkington TG, Hoffman J, Jaszczak RJ, MacFall JR, Harris CC, Kilts CD, Pelizzari CA, Coleman RE. Accuracy of surface fit registration for PET and MR brain images using full and incomplete brain surfaces. *J Comput Assist Tomogr*. 1995;19(1):117-124.
31. Friston KJ, Holmes AP, Worsley KJ, Poline JB, Frith CD, Frackowiak RSJ. Statistical parametric maps in functional imaging: a general linear approach. *Hum Brain Mapp*. 2004;2:189-210.
32. Kao CH, Ho YJ, Lan JL, Changlai SP, Liao KK, Chieng PU. Discrepancy between regional cerebral blood flow and glucose metabolism of the brain in systemic lupus erythematosus in patients with normal brain magnetic resonance imaging findings. *Arthritis Rheum*. 1999;42(1):61-68.
33. Warach S, Gur RC, Gur RE, Skolnick BE, Obrist WD, Reivich M. The reproducibility of the 133Xe inhalation technique in resting studies: task order and sex related effects in healthy young adults. *J Cereb Blood Flow Metab*. 1987;7(6):702-708.
34. Gur RC, Gur RE, Resnick SM, Skolnick BE, Alavi A, Reivich M. The effect of anxiety on cortical cerebral blood flow and metabolism. *J Cereb Blood Flow Metab*. 1987;7(2):173-177.
35. Romi F, Krakenes J, Aarli JA, Tysnes OB. Neuroborreliosis with vasculitis causing stroke-like manifestations. *Eur Neurol*. 2004;51(1):49-50.
36. Brogan GX, Homan CS, Viccellio P. The enlarging clinical spectrum of Lyme disease: Lyme cerebral vasculitis, a new disease entity. *Ann Emerg Med*. 1990;19(5):572-576.
37. Veenendaal-Hilbers JA, Perquin WV, Hoogland PH, Doornbos L. Basal meningovasculitis and occlusion of the basilar artery in two cases of Borrelia burgdorferi infection. *Neurology*. 1988;38(8):1317-1319.
38. Oksi J, Kalimo H, Marttila RJ, Marjamäki M, Sonninen P, Nikoskelainen J, Viljanen MK. Inflammatory brain changes in Lyme borreliosis: a report on three patients and review of literature. *Brain*. 1996;119(pt 6):2143-2154.
39. Morgen K, Martin R, Stone RD, Grafman J, Kadom N, McFarland HF, Marques A. FLAIR and magnetization transfer imaging of patients with post-treatment Lyme disease syndrome. *Neurology*. 2001;57(11):1980-1985.
40. Sackeim HA, Prohovnik I, Moeller J, Brown RP, Apter S, Prudic J, Devanand DP, Mukherjee S. Regional cerebral blood flow in mood disorders I: comparison of major depressives and normal controls at rest. *Arch Gen Psychiatry*. 1990;47(1):60-70.
41. Mayberg HS. Frontal lobe dysfunction in secondary depression. *J Neuropsychiatry Clin Neurosci*. 1994;6(4):428-442.
42. Drevets WC. Neuroimaging studies of mood disorders. *Biol Psychiatry*. 2000;48(8):813-829.